

Exchange integrals and magnetization distribution in $\text{BaCu}_2\text{X}_2\text{O}_7$ ($X=\text{Ge},\text{Si}$)S. Bertaina^{1,2} and R. Hayn¹¹Laboratoire Matériaux et Microélectronique de Provence, Faculté St. Jérôme, Case 142, F-13397 Marseille Cedex 20, France²Laboratoire de Magnétisme Louis Néel, CNRS, BP 166, 38042 Grenoble Cedex-09, France

(Received 17 November 2005; revised manuscript received 7 February 2006; published 12 June 2006)

Estimating the intrachain and interchain exchange constants in $\text{BaCu}_2\text{X}_2\text{O}_7$ ($X=\text{Ge},\text{Si}$) by means of density-functional calculations within the local spin-density approximation (LSDA) we find the Ge compound to be a more ideal realization of a one-dimensional spin chain with Dzyaloshinskii-Moriya interaction than its Si counterpart. Both compounds have a comparable magnitude of interchain couplings in the range of 5–10 K, but the nearest neighbor intrachain exchange of the Ge compound is nearly twice as large as for the Si one. Using the LSDA+ U method we predict the detailed magnetization density distribution and especially remarkable magnetic moments at the oxygen sites.

DOI: 10.1103/PhysRevB.73.212409

PACS number(s): 75.10.Pq, 71.15.Ap, 71.15.Mb, 71.20.Be

The study of low-dimensional magnetism is of broad interest, especially due to the crucial role of quantum fluctuations in those systems. To investigate quantum spin chains experimentally one needs low-dimensional model compounds. A representative example is $\text{BaCu}_2\text{Ge}_2\text{O}_7$,¹ or the isomorphous compound $\text{BaCu}_2\text{Si}_2\text{O}_7$,⁴ knowing to be the most ideal nonorganic spin chain compound exhibiting the Dzyaloshinskii-Moriya (DM)^{2,3} interaction. But why are some compounds more ideal than others? What are the remaining differences to an ideal one-dimensional compound? To answer these questions we present here a microscopic calculation of the electronic structure of $\text{BaCu}_2\text{X}_2\text{O}_7$ ($X=\text{Ge},\text{Si}$) within density-functional theory. We investigate the chemical trends in comparing the Ge with the Si compound, especially with respect to the intrachain and interchain tight-binding and exchange parameters. Furthermore, we calculate the magnetization density in detail.

$\text{BaCu}_2\text{Ge}_2\text{O}_7$ and $\text{BaCu}_2\text{Si}_2\text{O}_7$ were first synthesized and their crystallographic structures were described in 1993.⁵ Both are composed of CuO_4 nonideal plaquettes (the Cu atom and the four O atoms are not perfectly coplanar) which are arranged into corner-sharing chains along the c axis (see Fig. 1) but with a Cu-O-Cu bonding angle between 90 and 180 degrees. These bonding angles are $\phi=135^\circ$ (124°) for the Ge (Si) compound, and the zigzag chains allow for a DM interaction (due to the low crystallographic symmetry, space

group $Pnma$). Correspondingly, both compounds were intensively studied as examples for the influence of the DM interaction in quantum spin chains. A weak ferromagnetism was observed in the Ge compound⁶ which allows the experimental determination of the spin canting angle due to the DM interaction to be 1.9° . On the other hand, $\text{BaCu}_2\text{Si}_2\text{O}_7$ has attracted interest in connection with the finding of two consecutive spin reorientation transitions.^{7,8,10} Also, two gaps in the excitation spectrum of the Si compound had been found by neutron scattering⁹ and in antiferromagnetic resonance measurements.¹¹ These two gaps arise due to the DM interaction and the symmetric anisotropy term with a partial compensation between them.^{11,12} Recently, it was the Ge compound which allowed to test a prediction of Oshikawa and Affleck¹³ in good accuracy. The linewidth of the electron paramagnetic resonance signal diverges at low temperatures like $\Delta H \propto 1/T^2$ for an applied magnetic field perpendicular to the DM vector corresponding to the creation of a staggered field. But for an applied field parallel to the DM vector, when no staggered field can be created, the linewidth vanishes like $\Delta H \propto T$.¹

Despite all these results, a microscopic calculation which determines in detail the differences between the Si and the Ge compound is lacking up to now. It will be presented here. Our microscopic calculations confirm the naive expectation that the difference in the bonding angles is the main reason that the Ge compound is a better one-dimensional (1D) model system than the Si one. In addition, we also predict small oxygen moments in these compounds which should be detectable by several experimental methods.

Our analysis of exchange couplings and model parameters follows the lines given in Ref. 14 for Sr_2CuO_3 and Ca_2CuO_3 . We calculate the nonmagnetic band structure within the local density approximation (LDA) and perform a tight-binding (TB) analysis of the relevant band at the Fermi energy. Adding a Hubbard interaction term we may propose an effective one-band Hamiltonian which allows to estimate the different exchange terms. These are in reasonable agreement with total energy differences from the LSDA+ U method.

The scalar relativistic band-structure calculations were performed using the full potential local orbital (FPLO) method.¹⁵ In the FPLO method a minimum basis approach with optimized local orbitals is employed, being at the same

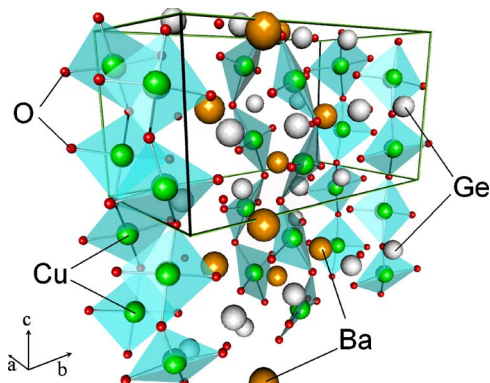


FIG. 1. (Color online) Crystal structure of $\text{BaCu}_2\text{Ge}_2\text{O}_7$. The crystal structure is $Pnma$. The chains run along the c axis.

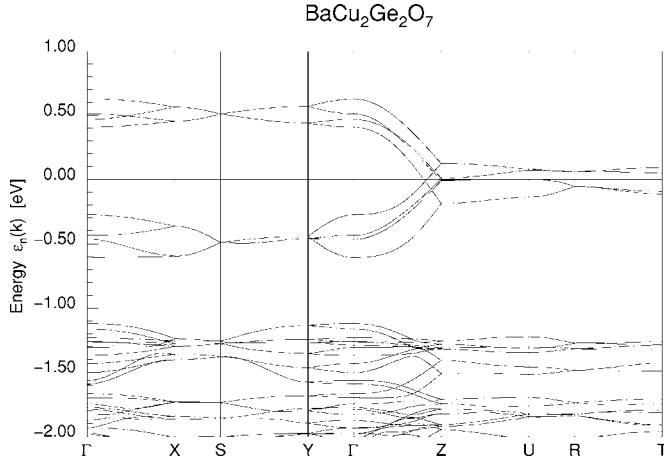


FIG. 2. Band structure of $\text{BaCu}_2\text{Ge}_2\text{O}_7$ within a nonmagnetic state using LDA. The momentum points in the Brillouin space are given in units of $(\pi/a, \pi/b, \pi/c)$ by $\Gamma=(0,0,0)$, $X=(1,0,0)$, $Y=(0,1,0)$, $Z=(0,0,1)$, $S=(1,1,0)$, $U=(1,0,1)$, $R=(1,1,1)$, and $T=(0,1,1)$. $\Gamma \rightarrow Z$ is the dispersion along the chain axis.

time a very accurate and an efficient numerical tool. For the present calculations we used the following basis set: Ba $4d5s5p : 6s6p$, Cu $3s3p : 4s4p3d$, Ge $3s3p : 4s4p; 3d5s$, Si $3s3p$, and O $2s2p; 3d$. The inclusion of the Ba $4d5s5p$ and the Cu $3s3p$ semicore states into the valence set was necessary to account for non-negligible core-core overlap, and the O $3d$ states were used to improve the completeness of the basis set. The site-centered potentials and densities were expanded in spherical harmonics up to $l_{\text{max}}=12$. The LDA calculations were performed using the Perdew-Wang parametrization.¹⁶ In all calculations we used a k -mesh of $4 \times 4 \times 4=64$ k -points in the Brillouin zone which is sufficient for the band-structure and magnetization density calculations reported below.

The nonmagnetic band structure of $\text{BaCu}_2\text{Ge}_2\text{O}_7$ is shown in Fig. 2. One may note a well isolated band at the Fermi level having eight branches according to the eight Cu ions per elementary cell (Fig. 1). The main valence band starts at about -1 eV and extends up to -7 eV. It is comprised of highly hybridized Cu $3d$ and O $2p$ orbitals as it is common for cuprate compounds.¹⁴ The band at the Fermi level consists mainly of the Cu $3d_{x^2-y^2}$ orbital lying predominantly within the plane of the CuO_4 plaquette (in the local plaquette coordinate system) and hybridizing slightly by $pd\sigma$ bonds with the oxygen $2p$ orbitals directed towards Cu. One must choose the nonmagnetic solution to determine the TB parameters¹⁴ since the Hubbard correlation will be added later on by hand. Taking into account nearest-neighbor hopping processes into all three Cartesian directions and providing a down-folding into the present Brillouin zone we may approximately describe the eight branches of the dispersion of the relevant band by

$$E_k = \pm 2t_z \cos\left(\frac{k_z c}{2}\right) \pm 2t_x \cos\left(\frac{k_x a}{2}\right) \pm 2t_y \cos\left(\frac{k_y b}{2}\right). \quad (1)$$

The corresponding fit gives the parameters listed in Table I. The errors are estimated by the evident deviations of the real

TABLE I. Collection of experimental data and theoretical model constants for $\text{BaCu}_2X_2\text{O}_7$ ($X=\text{Ge}, \text{Si}$).

	$\text{BaCu}_2\text{Ge}_2\text{O}_7$	$\text{BaCu}_2\text{Si}_2\text{O}_7$
ϕ	135°	124°
$4t_z=4t$	(950 ± 20) meV	(700 ± 45) meV
$4t_y$	(130 ± 15) meV	(85 ± 20) meV
$4t_x$	(130 ± 30) meV	(150 ± 30) meV
$J_{\text{exp}}=J$	$540 \text{ K}=46.5 \text{ meV}^a$	$280 \text{ K}=24.1 \text{ meV}^b$
$T_{N,\text{exp}}=T_N$	8.6 K^a	9.2 K^b
J_{\perp}^{emp}	3.6 K	4.1 K
U	4.8 eV	5.1 eV
t_{\perp}	$110\text{--}150 \text{ meV}$	$100\text{--}140 \text{ meV}$
J_{\perp}^{band}	$7.3\text{--}13.6 \text{ K}$	$5.7\text{--}11.1 \text{ K}$

^aReference 6.

^bReference 4.

band structure (Fig. 2) from Eq. (1). They correspond to additional hopping processes not taken into account in the simple model with only nearest-neighbor hopping. Comparing the Si with the Ge compound we may note a rough agreement with respect to the interchain hoppings. But, as can be also expected from the different bonding angles ϕ , the in-chain hopping is clearly enhanced for $\text{BaCu}_2\text{Ge}_2\text{O}_7$ in comparison to its Si counterpart.

We may use the derived TB parameters to construct a highly correlated one-band Hubbard model,

$$H = t \sum_{i,\pm z,\sigma} c_{i,\sigma}^+ c_{i\pm z,\sigma} + t_{\perp} \sum_{i,\pm x/y,\sigma} c_{i,\sigma}^+ c_{i\pm x/y,\sigma} + U \sum_i n_{i,\downarrow} n_{i,\uparrow}, \quad (2)$$

by identifying $t_z=t$ and using for t_{\perp} the average value of t_x and t_y . This Hubbard-type Hamiltonian may be further reduced to a Heisenberg one $H=(1/2)\sum_{i,j} J_{ij} \mathbf{S}_i \mathbf{S}_j$, where the exchange couplings are connected with the TB parameters by $J_{ij}=4t_{ij}^2/U$. Please note, that for the purpose of estimating the interchain couplings, we neglected those terms in the Hamiltonian which are the most interesting in the present case, namely the DM term and the symmetric anisotropy. They are caused by the spin-orbit coupling $\lambda \mathbf{S} \mathbf{L}$ ($\lambda \approx 0.1$ eV) and should be understood to be added to the isotropic part. A perturbative estimate leads to an orbital moment $\propto \lambda/\epsilon_d$ (ϵ_d , crystal field splitting of d levels) and a spin canting angle of 3° caused by the DM interaction $\propto \lambda$. The symmetric anisotropy $\propto \lambda^2$ compensates partly the DM term and it is just the Hund's rule coupling which leads to a "residual anisotropy" and to the two gaps in the magnetic excitation spectrum.¹¹

Experimental information about the nearest-neighbor exchange coupling J was derived from the maximum of the susceptibility curves^{4,6} using the Bonner-Fisher theory¹⁷ (see Table I). Using simply the same U for both compounds one would predict the ratio $J^{\text{Ge}}/J^{\text{Si}}=1.84$ from the theoretical $t=t_z$ values, which is already in good agreement with the experimental ratio 1.9. One can also take the experimental J values and the band-structure t 's to derive an effective one-

band Hubbard U of 4.8 eV (Ge) and 5.1 eV (Si) which seem to be quite reasonable (see Table I). In the given case the simple formula $J=4t^2/U$ works much better than for Sr_2CuO_3 or CuGeO_3 where considerable ferromagnetic corrections are necessary.¹⁴ Due to the zigzag chains the hopping t parameters of Table I are much smaller than for Sr_2CuO_3 which gives a better justification of the second order perturbation theory. On the other hand, the Cu ions are more far away from each other than in CuGeO_3 which reduces the direct ferromagnetic exchange contributions.

The theoretical interchain hopping and exchange parameters are connected with quite important error bars (which is, however, not unusual for cuprate compounds). One possibility to derive the magnetic interchain couplings was discussed above and leads to $J_{\perp}^{\text{band}}=4t_{\perp}^2/U$ (see Table I). Another method uses the theory of Irkhin and Katanin¹⁸ which is an improved Schulz theory¹⁹ of weakly coupled spin chains. It was recently confirmed by detailed quantum Monte Carlo calculations.²⁰ In the theory of Irkhin and Katanin, the Néel temperature T_N is given by

$$T_N = kJ_{\perp}z_{\perp}\tilde{\chi}_0L(\Lambda J/T_N) \quad (3)$$

with the numerical constants $k=0.70$, $\tilde{\chi}_0=2.1884$, $\Lambda=5.8$, the number of nearest neighbors $z_{\perp}=4$, and the scaling function

$$L(\Lambda J/T_N) = B \left(\ln \frac{\Lambda J}{T_N} + \frac{1}{2} \ln \ln \frac{\Lambda J}{T_N} \right)^{\frac{1}{2}} \quad (4)$$

with $B=0.15$. Applying (3) and (4) and using the measured values of $T_{N,\text{exp}}$ and J_{\perp}^{exp} we derived the empirical interchain exchange constants J_{\perp}^{emp} collected in Table I. Both methods lead to more or less identical interchain couplings for the two compounds. But the J_{\perp}^{band} are roughly a factor of 2 larger than the empirical values J_{\perp}^{emp} . A similar discrepancy had been already observed for Sr_2CuO_3 , Ca_2CuO_3 , and CuGeO_3 in Ref. 14, where also possible origins of that discrepancy had been discussed. Our present estimate gives only a rough idea about the absolute values of interchain couplings, but cannot answer whether these couplings would be ferromagnetic or antiferromagnetic. Certainly, a more precise determination of

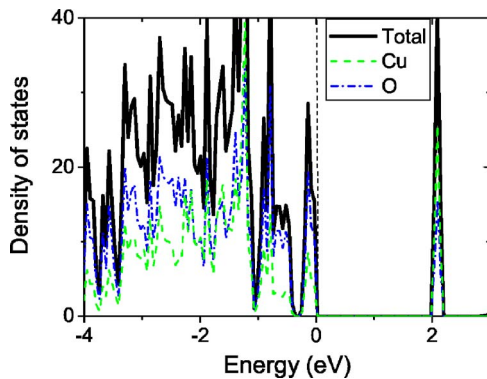


FIG. 3. (Color online) Total and partial density of states (DOS) of $\text{BaCu}_2\text{Ge}_2\text{O}_7$ from LSDA+ U calculation. The thick black line is the total DOS whereas the thin green and blue lines are the DOS of all copper and oxygen orbitals, respectively.

TABLE II. Distribution of magnetization in $\text{BaCu}_2X_2\text{O}_7$ with $X=\text{Ge, Si}$ using FPLO within the LSDA and the LSDA+ U schemes. Numerical values are in Bohr magneton.

	m_{Cu}	m_{O1}	m_{O2}	m_{O3}
LSDA				
$\text{BaCu}_2\text{Ge}_2\text{O}_7$	0.291	0.062	0.070	0.002
$\text{BaCu}_2\text{Si}_2\text{O}_7$	0.478	0.067	0.066	0.002
LSDA+ U				
$\text{BaCu}_2\text{Ge}_2\text{O}_7$	0.623	0.054	0.082	0.009
$\text{BaCu}_2\text{Si}_2\text{O}_7$	0.680	0.062	0.061	0.002

interchain couplings deserves more investigations.

By allowing an antiferromagnetic (AFM) arrangements of spins we found an insulating AFM solution already within the local spin-density approximation (LSDA). However, the obtained gap values of about 0.5 eV are unrealistically small in LSDA. Therefore, we performed LSDA+ U calculations with the Slater-Coulomb parameters $F_2=8.6$ eV, $F_4=5.4$ eV (corresponding to $J_H=1$ eV) and two values for $F_0=U=3.7$ eV and 5 eV. The former value produces gaps corresponding to the deep blue color of the samples (Fig. 3), but the latter one is more close to parameters common for cuprates.²¹ We used the same optimized basis orbitals like for the LSDA calculation and the “around mean field” version of LSDA+ U . The total energy differences between FM and AFM solution per magnetic ion ΔE lead to the nearest-neighbor exchanges $J=\Delta E/\ln 2$ of 46.6 (65.2) meV and 22.6 (45.5) meV for the Ge and Si compound with $U=5.0$ (3.7) eV.

The magnetization distribution on the different sites of the two compounds within LSDA and LSDA+ U (for $F_0=3.7$ eV having only small deviations to the $F_0=5$ eV solution) is shown in Table II.²² In the plaquette, each Cu ion is surrounded by four oxygens: O1 and O2 are the side oxygens, and O3 is the bridging oxygen between two plaquettes.

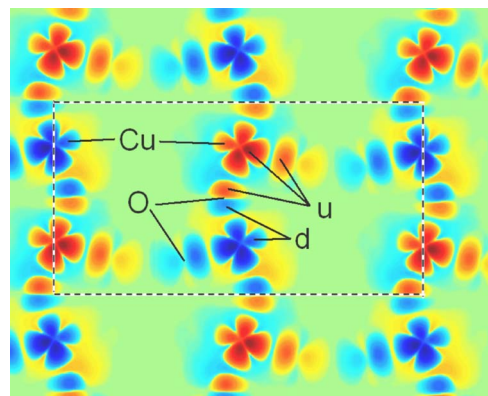


FIG. 4. (Color online) Local magnetization distribution of $\text{BaCu}_2\text{Ge}_2\text{O}_7$ in the bc plane passing through the vertical chain axis c . Shown is the spin density in a logarithmic scale: yellow to red (blue) parts correspond to spin up (u) [down (d)] density, green parts are very low local density. Dashed lines represent the elementary cell.

As one can see, a non-negligible part of the magnetization is situated at the oxygen sites, mainly at O1 and O2. Compared to the LSDA results, the proper inclusion of Coulomb correlations leads to an increase of magnetization at the Cu sites since it stabilizes the AFM long range order by decreasing the quantum fluctuations.

To see the magnetization distribution in more detail we calculated the spin density $n_{\uparrow} - n_{\downarrow}$ in real space within the elementary cell. It is presented in Fig. 4 in a logarithmic scale. We neglect here the small deviations from a collinear spin arrangement, which is justified by the small spin canting angle of 1° – 2° . One observes the characteristic form of $3d$ orbitals at the Cu sites and also the different oxygen sites. Quite remarkable are the different magnetization directions in the two lobes of the bridging oxygen, which explains the small numbers for m_{O3} . A sign change of the magnetization

at O3 is theoretically possible by sp hybridization. On the contrary, the magnetization points into one direction at the side oxygens.

Summarizing, we determined model parameters and predicted oxygen moments in $\text{BaCu}_2\text{X}_2\text{O}_7$ ($X=\text{Ge}, \text{Si}$). The absolute values of interchain couplings $|J_{\perp}|$ are very similar for $\text{BaCu}_2\text{Ge}_2\text{O}_7$ and $\text{BaCu}_2\text{Si}_2\text{O}_7$, but the nearest-neighbor intrachain J 's are different. The larger J for the Ge system makes it to be a more ideal model compound than $\text{BaCu}_2\text{Si}_2\text{O}_7$. Our calculated oxygen moments should be observable by ^{17}O nuclear magnetic resonance, by μ -spin rotation measurements, or by neutron scattering. They are similar (but slightly smaller) than those in Li_2CuO_2 which were recently detected.²³

The authors thank A. Stepanov and H. Rosner for interesting discussions.

-
- ¹S. Bertaina, V. A. Pashchenko, A. Stepanov, T. Masuda, and K. Uchinokura, Phys. Rev. Lett. **92**, 057203 (2004).
²I. Dzyaloshinskii, J. Phys. Chem. Solids **4**, 241 (1958).
³T. Moriya, Phys. Rev. **120**, 91 (1960).
⁴I. Tsukada, Y. Sasago, K. Uchinokura, A. Zheludev, S. Maslov, G. Shirane, K. Kakurai, and E. Ressouche, Phys. Rev. B **60**, 6601 (1999).
⁵J. A. S. Oliveira, Ph.D. thesis, Ruprecht-Karls-Universität, Heidelberg, 1993.
⁶I. Tsukada, J. Takeya, T. Masuda, and K. Uchinokura, Phys. Rev. B **62**, R6061 (2000).
⁷I. Tsukada, J. Takeya, T. Masuda, and K. Uchinokura, Phys. Rev. Lett. **87**, 127203 (2001).
⁸A. Zheludev, E. Ressouche, I. Tsukada, T. Masuda, and K. Uchinokura, Phys. Rev. B **65**, 174416 (2002).
⁹M. Kenzelmann *et al.*, Phys. Rev. B **64**, 054422 (2001).
¹⁰V. Glazkov and H.-A. Krug von Nidda, Phys. Rev. B **69**, 212405 (2004).
¹¹R. Hayn, V. A. Pashchenko, A. Stepanov, T. Masuda, and K. Uchinokura, Phys. Rev. B **66**, 184414 (2002).
¹²L. Shekhtman, O. Entin-Wohlman, and A. Aharony, Phys. Rev. Lett. **69**, 836 (1992).
¹³M. Oshikawa and I. Affleck, Phys. Rev. B **65**, 134410 (2002).
¹⁴H. Rosner, H. Eschrig, R. Hayn, S. L. Dreschsler, and J. Malek, Phys. Rev. B **56**, 3402 (1997).
¹⁵K. Koepf and H. Eschrig, Phys. Rev. B **59**, 1743 (1999).
¹⁶J. P. Perdew and Yu. Wang, Phys. Rev. B **45**, 13244 (1992).
¹⁷J. C. Bonner and M. E. Fisher, Phys. Rev. **135**, A640 (1964).
¹⁸V. Yu. Irkhin and A. A. Katanin, Phys. Rev. B **61**, 6757 (2000).
¹⁹H. J. Schulz, Phys. Rev. Lett. **77**, 2790 (1996).
²⁰C. Yasuda, S. Todo, K. Hukushima, F. Alet, M. Keller, M. Troyer, and H. Takayama, Phys. Rev. Lett. **94**, 217201 (2005).
²¹Please note that for the standard parameter set with $U=5$ eV the lowest unoccupied band of our calculation is of Cu $4s$ character in contrast to the expected Cu $3d$ orbital.
²²Only the spin moments; the orbital moments are expected to be of the order 0.05 – $0.1\mu_B$ as estimated from perturbation theory or calculated for the similar compound Li_2CuO_2 . D. Mertz, R. Hayn, I. Opahle, and H. Rosner, Phys. Rev. B **72**, 085133 (2005).
²³E. M. L. Chung, G. J. McIntyre, D. M. Paul, G. Balakrishnan, and M. R. Lees, Phys. Rev. B **68**, 144410 (2003).